Korean J. Chem. Eng., 40(1), 205-214 (2023)
DOI: 10.1007/s11814-022-1265-2

pISSN: 0256-1115
eISSN: 1975-7220

Downstream process development of biobutanol using deep eutectic solvent

Byoung Chul Kim*, Jin Whan Park, and Young Han Kim**,†**

*Dept. of Chem. & Energy Eng., Kyungnam Coll. of Info. & Tech., Busan 47011, Korea
**Dept. of Industrial Chemistry, Pukyong National University, Busan 48547, Korea
(*Received 19 April 2022 • Revised 13 June 2022 • Accepted 17 August 2022*)

Abstract−Biobutanol is produced from lignocellulose fermentation. Owing to the abundance of this feedstock and the similarities between the properties of biobutanol and gasoline, biobutanol represents a promising alternative to current crude-oil-based automotive fuel. Environmentally friendly recovery of biobutanol from the fermentation products is essential for achieving carbon-neutral production. Because extraction substantially lowers the energy demand for distillation, an eco-friendly deep eutectic solvent (DES) was applied for biobutanol extraction here, and the non-random two-liquid (NRTL) parameters that were compatible with the process design program were derived using experimental measurements and molecular simulations. For the liquid-liquid equilibrium (LLE) parameter estimation, a non-iterative procedure was introduced with a suitable arrangement of binary parameters for the DES. Compared to previous studies, the process design results indicate a marked reduction in energy consumption for the near-complete recovery of high-purity biobutanol, requiring a comparable investment.

Keywords: Biobutanol Recovery, Deep Eutectic Solvent, Extraction-distillation, Extractive Distillation, Energy-efficient

INTRODUCTION

Global concern regarding climate change has prompted the bio-production of various fuels and chemicals. The paradigm shift toward the usage of bioactive products in chemical industries implies the necessity for utilizing safe and appropriate techniques for product extraction from biomass or fermentation broths [1-5]. Green technology in the chemical processing industry encompasses the use of nonconventional solvents for extraction, an energy-efficient separation technique replacing distillation. Deep eutectic solvents (DESs) satisfy this requirement, and many studies on the thermodynamic properties of the liquid-liquid equilibrium (LLE) [6,7] and vapor-liquid equilibrium (VLE) [8,9] have provided basic developmental information on the extraction of bio-derived products, generally present in low quantity in water mixtures. Conventional processing requires a large amount of energy for water removal from the fermentation broth containing the bio-products. A DES composed of a hydrogen bond donor (HBD) and a hydrogen bond acceptor (HBA) can participate in complex intermolecular hydrogen-bonding interactions. In principle, the application of DESs for the processing of high-water-content bio-product mixtures is thermodynamically sustainable. The DES properties in the liquid state can be manipulated by selecting a pair of a HBD and HBA and adjusting their molar ratio of mixing to enable targeted extraction and azeotrope suppression during distillation.

In biobutanol production, an acetone-butanol-ethanol (ABE) mixture is produced from the fermentation of lignocellulose by *Clostridia* bacteria without pretreatment [10,11], while bioethanol is derived from edible grain or lignocellulose with pretreatment. Furthermore, the biobutanol is better in terms of energy content and it has close air-to-fuel ratio to gasoline [12]. However, the recovery of fermented biobutanol from aqueous media consumes more energy than bioethanol because of its low volatility, so a more complex process is needed to separate butanol from the ABE fermentation product [13]. To reduce the high energy demand, solvent extraction has been employed in the recovery process [14]. Oleyl alcohol, 1-octanol, 1-dodecanol, and 2-ethyl-1-hexanol are typical extractants [15], and 1-heptanol has been used most recently [16].

In this study, an eco-friendly solvent was employed for biobutanol recovery from an ABE broth, and a recovery process was introduced to separate acetone, butanol, and ethanol. The LLE and VLE models applied in the development of the recovery process were developed from experimental data and molecular simulations. The NRTL model parameters applied in the Aspen Plus simulation were arranged for an equimolar mixture of DES constituents. The performance of the proposed recovery process was evaluated in comparison with the results of previous reports. The study achieved the following: (i) a DES solvent was introduced for biobutanol extraction and purification; (ii) NRTL model parameters compatible to Aspen Plus ver. 8.8 were estimated using a non-iterative procedure; and (iii) a less-energy-consuming process compared to that of other processes was developed, requiring a comparable investment.

THERMODYNAMIC MODEL

When a chemical process is developed using design software, the applied thermodynamic model is essential for determining the equipment size and operating conditions. The accuracy of the process parameters predicted by the model must be evaluated against experimental and molecular simulation results.

1. Solvent Selection

To develop a biobutanol recovery process, design software uti-

†To whom correspondence should be addressed.
E-mail: yhkim2@pknu.ac.kr

lizes thermodynamic models of LLE and VLE for extractor and distillation column design, respectively; therefore, the accuracy of the model parameters derived from experimental measurements or estimated from molecular simulation results is key to determining the extraction solvent. When multiple sets of data are available, a better performing solvent is selected. In this study, a DES was developed, comprising DL-menthol as a HBD and decanoic acid as an HBA in equimolar amounts, and LLE measurements [17] and molecular simulations were applied to estimate the NRTL parameters in the process design. The menthol/decanoic acid combination exhibits high selectivity for butanol and ethanol, enabling high butanol and ethanol content in the organic phase, giving rise to a high distribution coefficient (Type II LLE). The LLE properties guide the design of an efficient extractor. In comparison to a similar DES system comprising menthol and palmitic acid at a molar ratio of 12 : 1 [6], the selection guidelines predicted a better extractive performance for the menthol/ decanoic acid pair.

2. NRTL Model

Although artificial neural networks were used in the property estimation of biofuel [18], their available database is not comparable to current models of thermodynamic property estimation. The NRTL model [19] is an activity coefficient model, widely utilized in process design [20-23] because activity coefficients are dependent on the composition of a given liquid system [24,25]. The activity coefficient of component *i* in the liquid phase is given by Eq. (1):

$$\ln\gamma_i = \frac{\sum_{j=1}^{N}\tau_{ji}G_{ji}x_j}{\sum_{k=1}^{N}G_{ki}x_k} + \sum_{j=1}^{N}\frac{x_jG_{ij}}{\sum_{l=1}^{N}G_{lj}x_l}\left[\tau_{ij} - \frac{\sum_{m=1}^{N}\tau_{mj}G_{mj}x_m}{\sum_{k=1}^{N}G_{kj}x_k}\right], \quad (1)$$

where N is the component number and x_j is the liquid composition (mole fraction) of component j. Using the binary interaction parameters a_{ji} and b_{ji}, and the non-randomness factor α_{ji}, the other parameters are derived as follows:

$$\tau_{ji} = a_{ji} + b_{ji}/T \quad (2)$$

$$G_{ji} = \exp(-\alpha_{ji}\tau_{ji}). \quad (3)$$

The activity coefficient for a given liquid composition in a ternary system can be calculated using a total of 15 binary interaction and non-randomness parameters. The existing studies on DES applications utilize two different methods for parameter assignment in Aspen Plus: introduction of a pseudo-component representing the DES comprising a mixture of a HBD and HBA solvent [6,23,26,27], or direct application of the constituent components [28]. The former requires estimated physical properties representing the mixture, while the latter requires thermodynamic equilibrium information for the HBD and HBA pair to estimate their binary parameters. The molar ratio of the DES pair is fixed in practical applications, and it is not an adjustable variable during process operation. Therefore, the equilibrium information between the pair is rarely available.

Among the various physical properties of the pseudo-component representing the DES mixture, the Antoine coefficient is critically important for estimating the binary parameters in VLE computation. The predicted vapor composition is determined from the following relation using the liquid composition x_i and activity coefficient γ_i. Although activity coefficients can be applied to a liquid, they are related to the vapor phase as follows:

$$\gamma_i x_i P_i = \varphi_i y_i P^T \quad (4)$$

where P_i is the pure component pressure, P^T is the total system pressure, φ_i is the fugacity coefficient, and y_i is the vapor composition (mole fraction) of component i. The pure component pressure is estimated from the Antoine equation, and the estimation accuracy depends on its coefficients. The coefficients of the pseudo-component are less reliable than those of the true components because component properties are estimated using various formulas with limited accuracy.

A new arrangement of NRTL parameters is proposed in this study. For a given molar ratio of a DES pair, their parameters are the same when paired with the other component, but zero when paired to each other, as listed in Table S1 of the Supplementary Material. Thermodynamically, the DES pair functions like a single component, as many studies have found that the NRTL prediction agrees well with the experimental measurements when they are treated as a pseudo-single-component [8,9]. However, this only applies for thermodynamic equilibrium estimation, and material and energy computations in process streams require additional physical properties, derived using less accurate data than the true components in the Aspen Plus database. Therefore, using the true components in the Aspen Plus application provides better process simulation than the pseudo-component replacements, and the thermodynamic equilibrium is accurately computed using the proposed arrangement of NRTL parameters, being the same for each component of the DES pair and zero between them. Note that the parameters are only valid for a given molar ratio of the DES pair.

3. LLE Parameters

The extraction of low-molecular-weight alcohols using a DES composed of DL-menthol and decanoic acid was experimentally evaluated [7], and the binary parameters of the NRTL model were estimated using a procedure modified from the conventional method, applying a non-iterative phase equation solution. Although the conventional K-value method [29] has been widely implemented for solving phase equations during parameter estimation [30], the associated iterative procedure consumes a considerable amount of time while the parameters are optimized for minimum estimation error.

The K-value method computes the compositions of the two liquid phases in equilibrium and satisfies the material balance and isoactivity conditions [29,31].

$$x_i^I = z_i/\{1 + (K_i - 1)L^{II}\} \quad (5)$$

$$x_i^{II} = K_i x_i^I \quad (6)$$

$$K_i = \gamma_i^I/\gamma_i^{II} \quad (7)$$

where z_i is the composition of the feed mixture of two equilibrium phases, L^{II} is the ratio of liquid II, and K_i is the equilibrium constant of component *i*, derived using the activity coefficients. In the K-value method, the feed composition is computed iteratively using the flash equation in the VLE calculations [29], whereas here it was obtained from the tie-line data in the LLE ternary diagram. When z_1 is set to a value between the liquid compositions measured in two phases, z_2 is determined using the two liquid compositions in equilibrium and the trigonometric relation, as demonstrated in

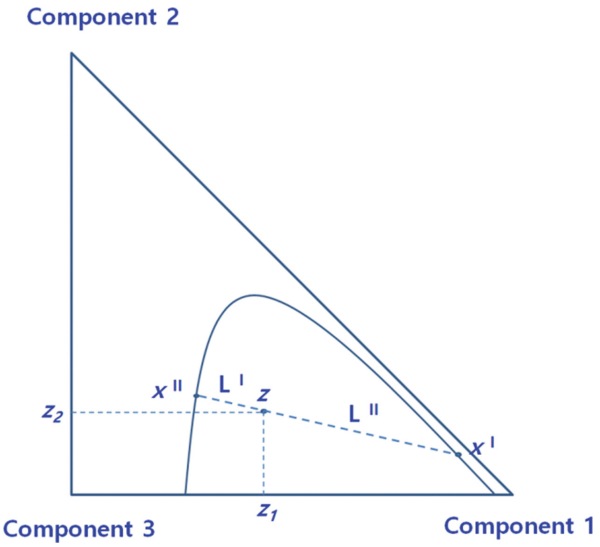

Fig. 1. Demonstration of feed composition calculation using tie-line liquid compositions.

Fig. 1. The diagram shows z_1 and z_2 in the same relation.

$$z_2 = x_2^I + (x_2^{II} - x_2^I)(x_1^I - z_1)/(x_1^I - x_1^{II}). \quad (8)$$

For a ternary mixture, the summation equation uses z_1 and z_2 to provide z_3. The fraction of liquid *II* is calculated using the lever rule:

$$L^{II} = (x_1^I - z_1)/(x_1^I - x_1^{II}). \quad (9)$$

Direct computation of the liquid fraction simplifies the conventional K-value method by eliminating the iterative calculations of Eqs. (5)-(7).

Therefore, the objective function in the parameter estimation of an LLE system becomes

$$\text{minimize} \quad f = \sum_{j=1}^{N_d} \sum_{k=1}^{N_p} \sum_{i=1}^{N_c} \left| x_{exp}^{i,k,j} - x_{pred}^{i,k,j} \right| \quad (10)$$

subject to

$$\min \quad \frac{\Delta G_{mix}}{RT} = \sum_{k=1}^{N_p} \sum_{i=1}^{N_c} l_i^k (\ln x_i^k + \ln \gamma_i^k), \quad (11)$$

where N_d, N_p, and N_c are the numbers of measured data points, phases, and components, respectively. Two liquid fractions are distinguished using L for the total fraction and *l* for the component fraction. The liquid *II* compositions were updated to minimize the Gibbs free energy of mixing (Eq. (11)), and the component fraction was determined using the total fraction and component composition [32]. R is the gas constant and T is the absolute temperature in K. The non-iterative solution of the phase equation simplifies the optimization of Eq. (10) compared to the conventional procedure.

4. VLE Parameters

Although experimental LLE data for a water/butanol/DES system used in this study are available, VLE data have not been obtained. However, many binary interaction parameters of the NRTL model are included in the database of the process design software used in this study, as listed in Table S1 of the Supplementary Material. Those not listed in the database were computed using molecular simulation. RASPA is an open software that calculates the molecular distribution between vapor and liquid phase boxes [33,34], and has been implemented in previous analogous studies [16,22,35-37]. The simulation results used for parameter estimation are listed in Table S2. Owing to the high viscosity of the DES solution, NRTL parameters derived from binary subsystems containing the DES could not accurately estimate the VLE behavior of ternary systems [8,38]. Therefore, the VLE parameters were estimated for a water/butanol/DES ternary system using the given binary parameters for the water/butanol subsystem in Aspen Plus database.

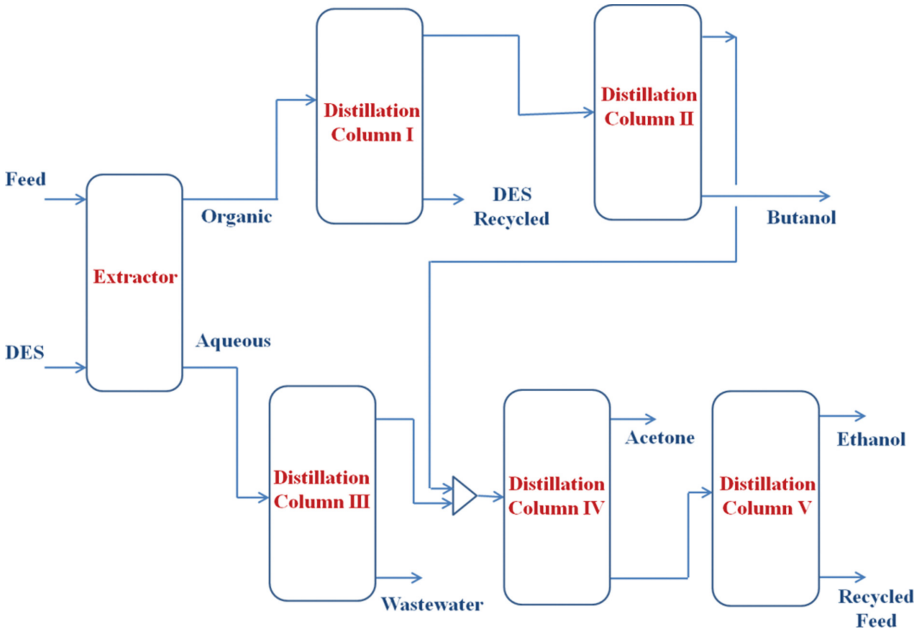

Fig. 2. A simplified schematic of the proposed biobutanol recovery process.

PROCESS DESIGN

The process proposed here is composed of an extractor that removes the bulk of the water from the fermented ABE feed, and distillation columns for product concentration. Fig. 2 presents an overview of the operational arrangement. The ABE feed parameters were sourced from a previous study [39], and the design capacity was given as 10,000 kg/h of feed. The unit processes were developed for product purity of 99% for acetone, 99% for butanol, and 94% for ethanol. The key operation of the overall process occurs in the extractor, wherein the ABE content in the extract and raffinate is determined, and subsequent processes depend on the ABE composition. As a significant amount of ABE remains in the raffinate, distillation is required to recover the ABE products. Owing to the large amount of water in the wastewater, the energy consumed by the distillation column constitutes a significant portion of the total consumed energy. Unlike other biofuel production processes, such as those of 2,3-butanediol [36] and ethanol [37], the current process includes wastewater distillation. The recovered ABE products and extract were distilled in five distillation columns to afford high-purity ABE products and recovered solvent. The column structural information was adopted from a published butanol process entailing the same feed and capacity [16], and the operating conditions were adjusted for the product specifications of this study. Aspen Plus [40] was implemented for the design.

RESULTS AND DISCUSSION

1. NRTL Parameters

The binary interaction parameters of the LLE NRTL model were largely derived from experimental measurements [7] using parameter estimation entailing non-iterative computation of the phase equation explained above. In the LLE system, the DES components dissolved slightly in water, and the resulting molar ratio was maintained throughout the process. Because Aspen Plus does not provide a single component representing the DES pair, several studies have introduced a pseudo-component with computed critical properties to replace the pair as a new component in process simulation. This component is used not only for the estimation of their thermodynamic properties, but also other physical properties, such as solubility and heat capacity. The use of true components in the Aspen Plus database leads to a more accurate estimation of the properties than achieved via pseudo-component estimation. By using the same parameters for the DES pair with other components and zero for their pair, the LLE computation treats the pair as a single component at any DES composition as long as their molar ratio remains the same. Experimental measurements of the LLE system were used in the extractor design as the binary parameters of the LLE NRTL thermodynamic model. An accurate process design is obtainable when the tie-line estimated using Aspen Plus is in good agreement with the experimental data. Fig. 3 illustrates the good agreement between the Aspen Plus estimation and the measured results, and includes the values estimated using the parameters listed in Table S1 of the Supplementary Material. In the experimental LLE measurements of the butanol/water/DES ternary system [6], the LLE of ethanol/water/DES was included, and the NRTL parameters were estimated using the same procedure as that used for the butanol system. In the case of acetone, no experimental data were available for the DES; therefore, the parameters provided by Aspen Plus were used in the study. Although less accurate predictions were expected for acetone recovery in the extractor, distillation column III recovered the acetone lost to the wastewater using the more accurate VLE parameters applied in the distillation column design.

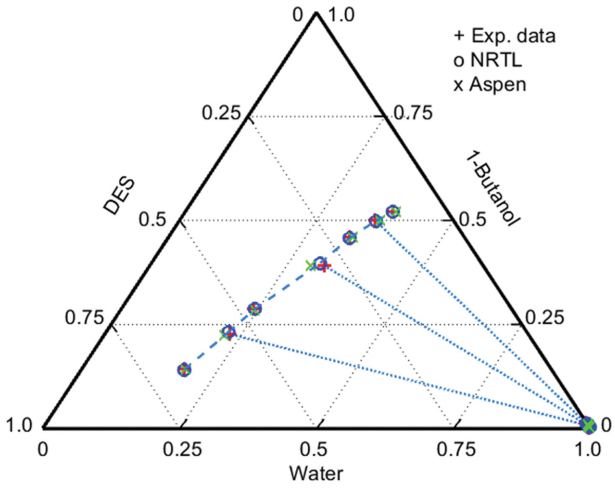

Fig. 3. Ternary diagram of the water/1-butanol/DES system. The plus symbols denote the experimental values, circles show the results computed by the NRTL model using the estimated parameters, multiplication symbols indicate Aspen Plus estimation, and the curves are predicted using the NRTL model. The DES is composed of DL-menthol and decanoic acid in an equimolar ratio.

Compared to the LLE system, the VLE NRTL parameters of binary pairs containing DES components have a less significant effect on distillation column simulation because their compositions in the distillation feed are negligible, except in the case of the solvent recovery column (Distillation Column I). Therefore, the VLE compositions were estimated using molecular simulation. Table S1 summarizes the parameters estimated using the simulation results listed in Table S2 in the Supplementary Material. Menthol and decanoic acid were treated as a single component, as explained above. The molar ratio of the pair remained nearly constant, because the high boiling points of the DES components confined them to the liquid phase. The distillation process involved in product separation was similar to that of a previously reported ABE recovery process [16]. The proposed component application in Aspen Plus was an attempt at improving the LLE prediction, and the same procedure was applied in very recent studies currently under review for publication. This procedure enabled a lower degree of deviation in property estimation compared with the current method.

While the butanol recovery process described in [7] was applied to a feedstock comprising 20 mol% butanol in water, that reported herein was designed for a much lower butanol content, coexisting with ethanol and acetone. Therefore, the entire recovery process was more complicated than that reported in the reference. Furthermore, the root-mean-square deviation (RMSD) for the composition predicted by the NRTL model in this study was 0.0028,

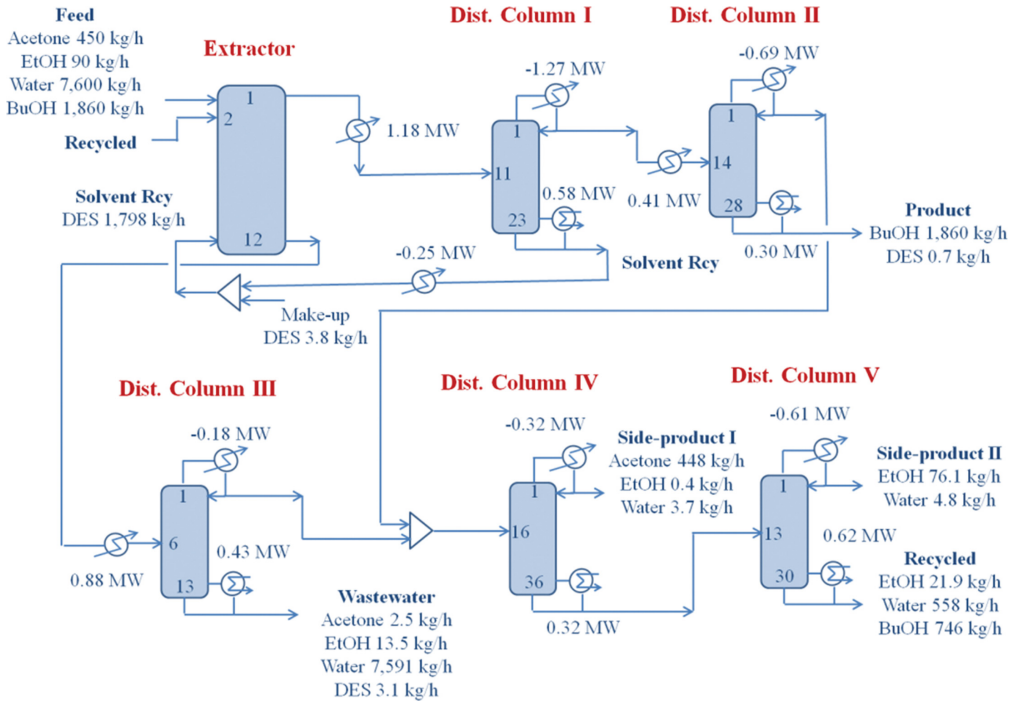

Fig. 4. A flow diagram of the proposed recovery process.

Table 1. Structural details and operating conditions of the proposed process. The tray numbers are counted from the top

Variable	Extractor	Dist. Col. I	Dist. Col. II	Dist. Col. III	Dist. Col. IV	Dist. Col. V
Structural						
Tray No.	12	23	28	13	36	30
Feed	1	11	14	6	16	13
Solvent	12					
Recycle	2					
Operating						
Pressure (MPa)- top	0.1	0.1	0.1	0.42	0.1	0.1
Temperature (°C)						
Overhead	25.8	102.9	90.2	112.5	55.8	78.2
Bottom	27.4	221.7	119.6	145.0	89.9	93.1
Feed (kg/h)	10,000	5,270	3,476	7,854	1,859	1,407
Solvent (kg/h)	1,798					
Make-up (kg/h)	3.8					
Recycle (kg/h)	1,326					
Product (kg/h)						
Overhead	5,270	3,476	1,615	244	452	80.9
Bottom	7,854	1,794	1,861	7,610	1,407	1,327
Reflux (kg/h)	-	5,213	2,099	842	2,159	2,548
Vap. boil up (kg/h)	-	6,310	1,881	740	875	1,789
Cooling duty (MW)	-	−1.27	−0.69	−0.18	−0.32	−0.61
Reboiler duty (MW)	-	0.58	0.30	0.43	0.32	0.62
Preheat/Cool (MW)	−0.25	1.18	0.41	0.88		
Comp. (mass frac.)						
Feed						
Butanol/Ethanol	0.186	0.4920	0.7459	0.0016	0.4013	0.5302
Product	Ovhd.	Ovhd.	Btm.	Ovhd.	Btm.	Ovhd.
Butanol/Ethanol	0.4920	0.7459	0.9996	0.0052	0.5302	0.9407

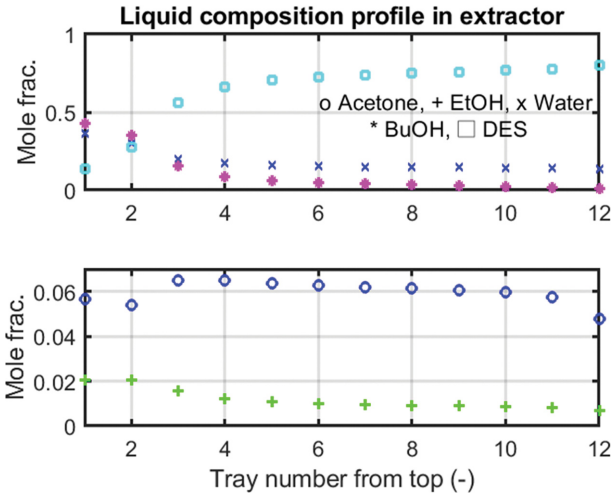

Fig. 5. Organic phase column profile in the extractor.

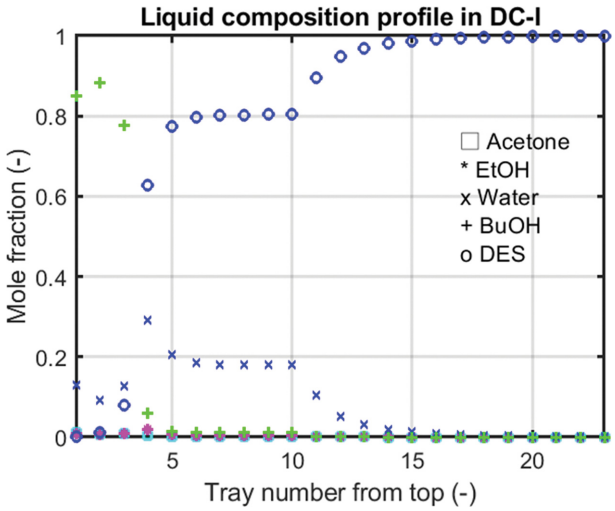

Fig. 6. Distillation column I profile; solvent is recovered at the bottom.

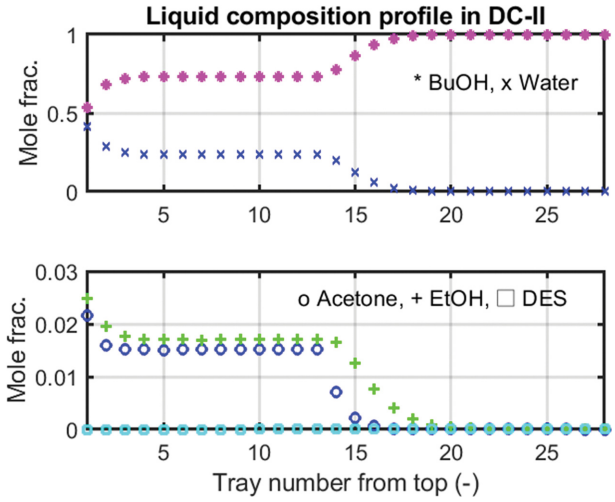

Fig. 7. Distillation column II profile; butanol is recovered at the bottom.

compared to 0.008 reported with the COSMO-ASPEN model in [7], indicating that the thermodynamic model entailing the proposed DES components and parameter estimation procedure was superior.

2. Process Design Results

The proposed process diagram, including the structural information of the unit processes with material and heat flows of major streams, is depicted in Fig. 4. The major product, butanol, was fully recovered at a purity of 99.96%, while the acetone and ethanol were recovered at recovery rates of 99.6% and 84.6%, and purities of 99.1% and 94.1%, respectively.

Further design details for the proposed process are summarized in Table 1. The extractor and distillation column tray numbers were taken from [16]. The column operating pressure was 1 bar, with the exception of distillation column III, in which the top tray pressure was raised to 4.2 bar for heat recovery from the large amount of wastewater. The pressure increase did not necessitate a significant increase in the column fabrication cost [41].

The composition of the organic phase in the extractor is illustrated in Fig. 5. The organic phase was removed at the top of the extractor to be processed further for butanol recovery. While the butanol, acetone, and ethanol compositions were high at the top, the DES composition was low. The role of the extractor is water removal from the feed and recycled stream; 93% of the water was separated into the raffinate in the extractor along with some product and solvent. The bulk of the acetone, 61% of ethanol, and all of the butanol were recovered from the raffinate as an overhead product of distillation column III. The final wastewater content, drawn as the bottom product, is shown in Fig. 4.

The liquid composition profile at the subsequent distillation column processing the extract to separate the solvent for recycling is shown in Fig. 6. The DES composition was the highest at the bottom, while the product and water compositions were high at the top of the column. Owing to the large difference between the DES and product boiling points, a sudden increase in DES composition was observed near the top of the column, as shown in the figure. The profile indicates that highly pure DES was obtained at the bottom of distillation column I. Water was the only contaminant at a concentration of 40 ppm in the recycled solvent. Another column profile of importance is that of distillation column II, shown in Fig. 7. This column produces butanol as the bottom product. Water and the two side products contained in the extract were separated as the overhead product. Because butanol and water have an azeotrope at 24 mol% butanol, butanol is contained in the overhead product and recycled to the extractor as a feed. Impurity accumulation during recycled solvent use is inevitable and, therefore, a small amount of the solvent must be purged to remove the built-up impurities [22]. However, freshly made solvent can be added to replace the purged amount, depending on the nature of the accumulated impurities.

3. Performance Evaluation

In addition to the objective of eco-friendly solvent utilization, energy conservation was another important goal of the study, and heat integration utilizing recovered heat was included in the pro-

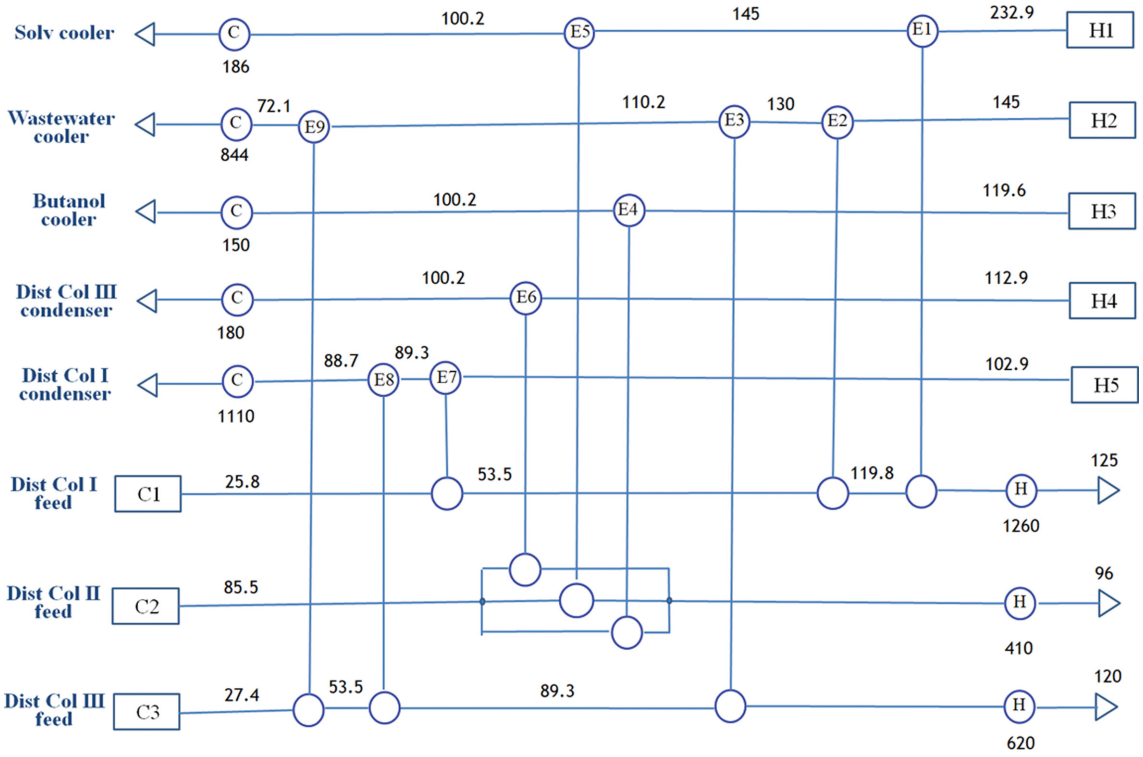

Fig. 8. A diagram of the heat exchanger network. Numbers below the circles represent the heat transfer rate in kW, and the numbers on the lines indicate the temperature in centigrade.

Table 2. Comparison of the energy requirements of previously studied biobutanol recovery processes

Process	Solvent	Feedstock (wt%)	Reboiler duty (MW) for butanol t/h	Remark	Ref.
Distillation		0.51	5.32	Heat integrated	[50]
Extr./Distil.	2-Et. hexanol	0.51	1.69	Heat integrated	[50]
Extr./Distil.	Hexyl acetate	14.29	16.9		[51]
Distillation		18.6	4.56		[39]
Distillation		18.6	1.72	Heat integrated	[39]
Distillation		0.8	7.11		[52]
Extr./Distil.	Mesitylene	0.8	1.33	Heat integrated	[52]
Extr./Distil.	Heptanol	18.6	1.02	Heat integrated	[16]
Extr./Distil.	Menthol/decanoic acid	18.6	1.21	Heat integrated	This study

cess design. The hybrid extraction/distillation process consumes considerably less energy compared to conventional distillation-only recovery processes, and additionally, heat recovery is achieved by introducing preheaters in the feed streams of distillation columns I, II, and III. The recovered heat sources were the recycled solvent cooler, wastewater cooler, butanol cooler, and condensers of distillation columns. A heat exchanger network was assembled using pinch technology [42] was utilized to evaluate the heat availability with a pinch temperature of 10 °C. Fig. 8 shows the heat exchanger network of nine units with four input and output stream temperatures at each unit. The heat duty of the developed process is 16% lower than the average consumption reported in previous studies, excluding excessively high-energy-consuming processes, as listed in Table 2.

The equipment and operational costs of the proposed process are listed in Table 3. The operating cost was calculated for 7,200 h/y operation at 10,000 kg/h feed with costs of $24/t and $21.3/1,000t for the steam and cooling water, respectively. The equipment costs included the column internal and heat exchanger costs, and were calculated using the cost equations [41,43-45] listed in Procedure P1 of the Supplementary Material. The cost of the proposed process is compared with those of reported processes in Table 4. The investment required for the proposed process was 5% higher than the average cost of 4 reported processes when a scaling-up exponent of 0.68 was applied for their production capacity [46].

The LLE composition in the aqueous phase of the water/butanol/DES system resulted in a relatively large amount of solvent being wasted in the extraction process. Because fermentation consumes

Table 3. Economic assessment of the proposed process. The units are in million U.S. dollars and the utility cost is per annum

Variable	Extractor	Dist. I	Dist. II	Dist. III	Dist. IV	Dist. V
Investment						
Column	0.129	0.162	0.139	0.061	0.134	0.148
Tray	0.007	0.008	0.007	0.002	0.006	0.007
Condenser		0.254	0.171	0.071	0.104	0.157
Reboiler		0.080	0.052	0.066	0.054	0.084
Preheater/cooler		0.127	0.064	0.105		
Subtotal	0.136	0.631	0.433	0.305	0.298	0.396
Total						2.199
Utility						
Steam		0.216	0.112	0.160	0.119	0.231
Coolant		0.017	0.009	0.002	0.004	0.008
Subtotal		0.233	0.121	0.163	0.123	0.239
Total						0.879

Table 4. The investment cost of the present process compared to the averaged costs of four reported processes. The units are in million U.S. dollars. Investment is normalized to the production capacity of this study with a scaling-up exponent of 0.68 [46]

Process	Investment	Solvent	Remark	Ref.
Distillation	2.33			[39]
Distillation	2.01		Heat integrated	[39]
Extraction/Distillation	1.85	Mesitylene	Heat integrated Wastewater, 76% water	[52]
Extraction/Distillation	2.20	Heptanol	Heat integrated	[16]
Extraction/Distillation	2.20	Menthol/Decanoic acid	Heat integrated	This study

large amounts of water and the solvent used in this study is bio-friendly, recycling the wastewater for use in fermentation minimizes solvent loss and water consumption.

Because the butanol content in the feedstock was low, the extraction performance of the DES affected the overall performance of the process the most. A low extraction recovery implies a large butanol loss in the wastewater, increasing its load in the subsequent distillation process. Therefore, DES selection is critical, and a less effective DES results in poor performance, although the proposed process is applicable to other DES systems.

Decanoic acid is corrosive to ASTM 304 stainless steel at a rate of 21 mg/m^2 h [47]. ASTM 317L is the type of stainless steel suggested for use with fatty acids at elevated temperatures [48]. When the DES was applied, the corrosion rate on the metal surface decreased with increased exposure owing to the formation of an oxidized layer between the metal strip and DES [49].

CONCLUSIONS

With the phasing out of fossil fuels, various biofuels are being increasingly utilized in automobiles. Biobutanol is preferred to bioethanol due to the abundance of lignocellulose as feedstock and its similarity to gasoline. A new energy-efficient hybrid extraction/distillation recovery process for fermented butanol is proposed, utilizing menthol/decanoic acid as a bio-friendly deep eutectic solvent and its performance was evaluated. Non-iterative estimation of the thermodynamic model parameters was introduced, and the compatibility of the estimated parameters with a commercial process design program was examined. The process design results indicated that butanol was fully recovered at a purity of 99.96%, and acetone and ethanol were recovered at recovery rates of 99.6% and 84.6% in purities of 99.1% and 94.1%, respectively. The energy requirement of the proposed process was substantially less than those of previously studied processes, yet with comparable investment costs.

ACKNOWLEDGEMENTS

We would like to thank Professor Yongchul G. Chung of Pusan National University for advising the RASPA implementation.

NOMENCLATURE

a : binary interaction parameter [-]
b : binary interaction parameter [-]
G : Gibbs free energy or defined in Eq. (3) [Jmol^{-1}]
K equilibrium constant [-]
L : liquid fraction [-]
l : component liquid fraction [-]
N : number of components or phases [-]
P : pressure [Pa]
R : ideal gas constant [Jmol^{-1}K^{-1}]
T : absolute temperature [K]
x : liquid composition [-]
z : feed composition [-]

Greek Letters

α : non-randomness parameter [-]
γ : activity coefficient [-]
τ : defined in Eq. (2) [-]
φ : fugacity coefficient [-]

Superscripts

I : liquid I
II : liquid II
T : total system

Subscripts

c : component number
i : component i
j : component j
k : component k
l : component l
m : component m
p : phase number

SUPPORTING INFORMATION

Additional information as noted in the text. This information is available via the Internet at http://www.springer.com/chemistry/journal/11814.

REFERENCES

1. D. Kushwaha, N. Srivastava, I. Mishra, S. N. Upadhyay and P. K. Mishra, *Rev. Chem. Eng.*, **35**, 475 (2019).
2. G. Fomo, T. N. Madzimbamuto and T. V. Ojumu, *Sustainability*, **12**, 5244 (2020).
3. K. A. Baritugo, J. N. Son, Y. J. Sohn, H. T. Kim, J. C. Joo, J. I. Choi and S. J. Park, *Korean J. Chem. Eng.*, **38**, 1291 (2021).
4. E. B. D'Alessandro, A. T. Soares, R. G. Lopes, R. B. Derner and N. R. Antoniosi, *Chem. Eng. Commun.*, **208**, 965 (2021).
5. S. Kang, M. J. Realff, Y. H. Yuan, R. Chance and J. H. Lee, *Korean J. Chem. Eng.*, **39**, 1524 (2022).
6. R. Verma and T. Banerjee, *Glob. Chall.*, **3**, 1900024 (2019).
7. R. Verma, P. K. Naik, I. Diaz and T. Banerjee, *Fluid Phase Equilibr.*, **533**, 112949 (2021).
8. Y. Peng, X. Lu, B. Liu and J. Zhu, *Fluid Phase Equilibr.*, **448**, 128 (2017).
9. G. A. L. Souza, L. Y. A. Silva and P. F. M. Martinez, *J. Chem. Thermodyn.*, **158**, 106444 (2021).
10. H. Amiri and K. Karimi, *Bioresour. Technol.*, **270**, 702 (2018).
11. R. N. Menchavez and S. H. Ha, *Korean J. Chem. Eng.*, **36**, 909 (2019).
12. H. Amiri, K. Karimi and H. Zilouei, *Bioresour. Technol.*, **152**, 450 (2014).
13. A. Calhan, S. Deniz, J. Romero and A. Hasanoglu, *Korean J. Chem. Eng.*, **36**, 1489 (2019).
14. P. Ibarra-Gonzalez, L. P. Christensen and B. G. Rong, *Chem. Eng. Commun.*, **209**, 529 (2021).
15. B. Bharathiraja, J. Jayamuthunagai, T. Sudharsanaa, A. Bharghavi, R. Praveenkumar, M. Chakravarthy and D. Yuvaraj, *Renew. Sust. Energy Rev.*, **68**, 788 (2017).
16. H. W. Oh, S. C. Lee, H. C. Woo and Y. H. Kim, *Chem. Eng. Technol.*, **44**, 2316 (2021).
17. K. Paduszyński, M. Więckowski, M. Okuniewski and U. Domańska, *J. Mol. Liq.*, **286**, 110819 (2019).
18. P. F. Arce, D. H. P. Guimaraes and L. R. de Aguirre, *Chem. Eng. Commun.*, **206**, 1273 (2021).
19. H. Renon and J. M. Prausnitz, *AIChE J.*, **14**, 135 (1968).
20. D. Jha, M. B. Haider, R. Kumar and M. S. Balathanigaimani, *Chem. Eng. Res. Des.*, **111**, 218 (2016).
21. L. H. Wu, L. Wu, Y. S. Liu, X. Q. Guo, Y. F. Hu, R. Cao, X. Y. Pu and X. Wang, *Chem. Eng. Res. Des.*, **129**, 197 (2018).
22. H. C. Woo and Y. H. Kim, *AIChE J.*, **65**, e16665 (2019).
23. X. Shang, S. Ma, Q. Pan, J. Li, Y. Sun, K. Ji and L. Sun, *Chem. Eng. Res. Des.*, **148**, 298 (2019).
24. S. H. Saravi, A. Ravichandran, R. Khare and C. C. Chen, *AIChE J.*, **65**, 1315 (2019).
25. S. Tanveer and C. C. Chen, *AIChE J.*, **66**, (2020).
26. N. R. Mirza, N. J. Nicholas, Y. Wu, S. Kentish and G. W. Stevens, *J. Chem. Eng. Data*, **60**, 1844 (2015).
27. H. Dongmin and C. Yanhong, *Chem. Eng. Process.*, **131**, 203 (2018).
28. G. Shu, Y. Tan, L. Cui, Y. Zhang and L. Zhang, *J. Chem. Eng. Data*, **65**, 3029 (2020).
29. M. L. Michelsen, *Fluid Phase Equilibr.*, **9**, 2 l (1982).
30. A. Marcilla, J. A. Reyes-Labarta and M. M. Olaya, *Fluid Phase Equilibr.*, **433**, 243 (2017).
31. Z. Li, K. A. Mumford, K. H. Smith, J. Chen, Y. Wang and G. W. Stevens, *Ind. Eng. Chem. Res.*, **55**, 2852 (2016).
32. F. Denes, P. Lang and M. Lang-Lazi, *IChemE Symposium Series. Inst. Chem. Eng., London.*, **152**, 877 (2006).
33. D. Dubbeldam, S. Calero, D. E. Ellis and R. Q. Snurr, raspa_instruction.pdf https://github.com/numat/RASPA2/blob/master/Docs/raspa.pdf (2015). (accessed on April 15, 2022).
34. D. Dubbeldam, S. Calero, D. E. Ellis and R. Q. Snurr, *Mol. Simul.*, **42**, 81 (2016).
35. C. H. Seo and Y. H. Kim, *Sep. Purif. Technol.*, **209**, 1 (2019).
36. S. C. Lee, H. C. Woo and Y. H. Kim, *Chem. Eng. Process.*, **160**, 108286 (2021).
37. S. C. Lee, H. C. Woo and Y. H. Kim, *Fuel*, **310**, 122393 (2022).
38. N. R. Rodríguez, A. S. B. González, P. M. A. Tijssen and M. C. Kroon, *Fluid Phase Equilibr.*, **385**, 72 (2015).
39. I. Patrascu, C. S. Bildea and A. A. Kiss, *Sep. Purif. Technol.*, **177**, 49 (2017).
40. Aspentech, Aspen Technology, Inc., Bedford. MA (2015).
41. J. M. Douglas, *Conceptual design of chemical processes*, McGraw-Hill, New York (1988).
42. I. C. Kemp, *Pinch analysis and process integration*, 2nd ed., Butterworth-Heinemann, Burlington, MA (2007).
43. R. Turton, R. C. Baille, W. B. Whiting and J. A. Shaeiwitz, *Analysis, synthesis, and design of chemical processes*, 2nd ed., Prentice Hall, Upper Saddle River, New Jersey (2003).
44. Z. Olujic, L. Sun, A. de Rijke and P. J. Jansens, *Energy*, **31**, 3083 (2006).
45. Y. H. Kim, *Energy*, **70**, 435 (2014).
46. A. Aden, M. Ruth, K. Ibsen, J. Jechura, K. Neeves, J. Sheehan, B. Wallace, L. Montague, A. Slayton and J. Lucas, National Renewable Energy Laboratory, Golden, CO (2002).

47. Q. Yan, G. Ma and W. Wang, *J. Phys.: Conf. Ser.*, **2076**, 012037 (2021).
48. Sandvik, Sandvik AB, Sandviken, Sweden, https://www.materials.sandvik/en/materials-center/corrosion-tables/fatty-acids/ (2022).
49. H. Ayaz, V. Chinnasamy and H. Cho, *Materials*, **14**, 7418 (2021).
50. M. Aneke and J. Gorgens, *Fuel*, **150**, 583 (2015).
51. C. A. Contreras-Vargas, F. I. Gomez-Castro, E. Sanchez-Ramirez, J. G. Segovia-Hernandez, R. Morales-Rodriguez and Z. Gamino-Arroyo, *Chem. Eng. Technol.*, **42**, 1088 (2019).
52. K. Kraemer, A. Harwardt, R. Bronneberg and W. Marquardt, *Comput. Chem. Eng.*, **35**, 949 (2011).

Supporting Information

Downstream process development of biobutanol using deep eutectic solvent

Byoung Chul Kim*, Jin Whan Park, and Young Han Kim**,†**

*Dept. of Chem. & Energy Eng., Kyungnam Coll. of Info. & Tech., Busan 47011, Korea
**Dept. of Industrial Chemistry, Pukyong National University, Busan 48547, Korea
(*Received 19 April 2022 • Revised 13 June 2022 • Accepted 17 August 2022*)

Procedure P1. Cost estimation equations for distillation column design.

The column costs were calculated using Eqs. (S1)-(S6) from references [44] and [45].

$$C_{col}=\left(\frac{M\ \&\ S}{280}\right)C_f D_C^{1.066} H_C^{0.802} C_p, \quad \text{(S1)}$$

where the Marshall and Swift (M&S) index=1,638.2, according to the latest available data. The fabrication factor C_f=3,919.32 and the pressure factor C_p is obtained from reference [41]. The diameter D_c [m] was calculated from the vapor flow according to Eq. (S2).

$$D_c = 0.08318\sqrt{V} \quad \text{(S2)}$$

where V [kmol/h] is the vapor flow. Column height was calculated using 2-feet spacing and number of trays. The internal

Table S1. Binary interaction parameters in the NRTL models

System	Component i	Component j	a_{ij}	a_{ji}	b_{ij}	b_{ji}	α	Ref.
LLE	Water	Acetone	0.0544	6.3981	419.9716	−1,808.99	0.3	[40]
	Water	Ethanol	0	0	721.3	−21.8	0.3	[7]
	Water	Butanol	0	0	1,541.6	−257.4	0.2	[7]
	Water	Menthol	0	0	2,825.4	272.5	0.2	[7]
	Water	DecaAcid	0	0	2,825.4	272.5	0.2	[7]
	Acetone	Ethanol	−0.3471	−1.0787	206.5973	479.05	0.3	[40]
	Acetone	Butanol	−8.8875	10.2979	3,077.281	−3,326.54	0.3	[40]
	Acetone	Menthol	0	0	657.6335	−381.339	0.3	UNIFAC
	Acetone	DecaAcid	0	0	657.6335	−381.339	0.3	
	Ethanol	Butanol	0	0	−85.2188	128.5015	0.3	[40]
	Ethanol	Menthol	0	0	361.4	75.7	0.3	[7]
	Ethanol	DecaAcid	0	0	361.4	75.7	0.3	[7]
	Butanol	Menthol	0	0	−285.1	823.96	0.3	[7]
	Butanol	DecaAcid	0	0	−285.1	823.96	0.3	[7]
	Menthol	DecaAcid	0	0	0	0	0.3	
VLE	Water	Acetone	0.0544	6.3981	419.9716	−1,808.99	0.3	[40]
	Water	Ethanol	3.4578	−0.8009	−586.081	246.18	0.3	[40]
	Water	Butanol	13.1102	−2.0405	−3,338.95	763.8692	0.3	[40]
	Water	Menthol	0	0	−1073.3	821.9	0.3	MD
	Water	DecaAcid	0	0	−1073.3	821.9	0.3	MD
	Acetone	Ethanol	−0.3471	−1.0787	206.5973	479.05	0.3	[40]
	Acetone	Butanol	−8.8875	10.2979	3,077.281	−3,326.54	0.3	[40]
	Acetone	Menthol	0	0	127.2	73.5	0.3	MD
	Acetone	DecaAcid	0	0	127.2	73.5	0.3	MD
	Ethanol	Butanol	0	0	−85.2188	128.5015	0.3	[40]
	Ethanol	Menthol	0	0	1,610.2	−912.2	0.3	MD
	Ethanol	DecaAcid	0	0	1,610.2	−912.2	0.3	MD
	Butanol	Menthol	0	0	311.5	667.9	0.3	MD
	Butanol	DecaAcid	0	0	311.5	667.9	0.3	MD
	Menthol	DecaAcid	0	0	0	0	0.3	

Table S2. Calculated compositions of vapor-liquid equilibrium in a system of water(1)/1-butanol(2)/DES(3) using molecular simulation. Units are in mole fraction

Temperature (K)	Liquid phase			Vapor phase		
	x_1	x_2	x_3	y_1	y_2	y_3
392.0	0.0711	0.8329	0.0960	0.0232	0.9696	0.0072
389.5	0.1096	0.7673	0.1231	0.1411	0.8543	0.0046
384.5	0.1255	0.7933	0.0812	0.2559	0.7441	0.0000
385.0	0.1373	0.7848	0.0779	0.2421	0.7579	0.0000
381.5	0.1494	0.7845	0.0661	0.3511	0.6489	0.0000
379.5	0.1645	0.7708	0.0647	0.3940	0.6060	0.0000
383.0	0.2483	0.5478	0.2039	0.4349	0.5584	0.0067
382.5	0.2637	0.5365	0.1998	0.4323	0.5605	0.0072
371.5	0.3412	0.5371	0.1217	0.6570	0.3430	0.0000
374.5	0.4070	0.3483	0.2447	0.7906	0.1940	0.0154
370.0	0.4329	0.3700	0.1971	0.7991	0.1954	0.0055
379.0	0.3733	0.3134	0.3133	0.7710	0.2206	0.0084
389.5	0.5320	0.0232	0.4448	0.9597	0.0101	0.0302

expense was determined from Eq. (S3):

$$C_{tray}=\left(\frac{M\ \&\ S}{280}\right)97.243D_C^{1.55}H_CF_c, \quad (S3)$$

where the factor F_c is taken from ref. [44]. The cost of heat exchanger is given as

$$C_{cond}=\left(\frac{M\ \&\ S}{280}\right)1{,}609.13A_C^{0.65}, \quad (S4)$$

where A_c is the heat transfer area of a condenser, defined by Eq. (S5):

$$A_c=\frac{Q_c}{U_c\Delta T}, \quad (S5)$$

where Q_c [W] is the heat transfer rate, U_c is the overall heat transfer coefficient, and ΔT is the temperature difference. The overall heat transfer coefficients for cooling and heating are 0.8 and 1.0 kW/m^2·K, respectively. The temperature differences were 10 K and 25 K for cooling and heating, respectively. Likewise, the reboiler cost is calculated as:

$$C_{reb}=\left(\frac{M\ \&\ S}{280}\right)1{,}775.26A_R^{0.65}, \quad (S6)$$

where A_R is the reboiler's heat transfer area. Costs of cooling water and steam were \$21.3/1,000t and \$23.97/t, respectively, with heat capacities of 11.62 kW/t (water) and 0.463 MW/t (steam) [43].